Paper III

The Role of the Support in Cr/oxide Catalysts for Dehydrogenation of Ethane

Sindre Lillehaug[a] and Knut J. Børve[a]

(Dated: April 10, 2006)

Dehydrogenation of ethane over Cr(III)/oxide has been explored by quantum chemical methods in conjunction with cluster models. This includes determining stationary geometries and energies for two reaction mechanisms that involve C–H activation by σ-bond metathesis. The surface models cover both alumina, silica and chromia supports and chromium bonded to the surface by either two or three oxygen bridges. In the case of silica, both mononuclear and dinuclear chromium were considered, whereas only mononuclear chromium was included for alumina. The computed energy profiles are used to discuss the role of the support and how it affects the activity of chromium with respect to dehydrogenation.

Keywords: Cr/alumina,ethane,dehydrogenation,DFT,cluster,surface catalyst, support, silica

I. INTRODUCTION

Increasing availability of low-cost feedstock of short alkanes has spurred a vast field of research into catalysts for dehydrogenation. [1, 2] Known catalysts fall into two groups, molecular transition-metal complexes [3] and surface catalysts. The latter class includes finely dispersed metallic platinum [4–6] and the system of interest in this contribution: Chromium supported on oxides such as silica, zirconia, titania and chromia. [1]

The catalytic activity of chromium with respect to dehydrogenation is reported to depend on the choice of oxide carrier as Cr/zirconia > Cr/alumina > Cr/silica > α-chromia. [7–11] There are several ways in which the carrier oxide may affect the observed catalytic activity. On the one hand, it is conceivable that different oxides may be able to stabilize different catalytically active species and hence support different mechanisms of dehydrogenation. On the other hand, the effect of the carrier may be through small modifications of one and the same reaction mechanism, leading to changes in the kinetic parameters only. Even if the same chromium species were active on all the relevant oxides, the oxides may still be able to stabilize the active species to a varying extent, thus effectively changing the concentration of the active chromium. A variation on the last point would be through the ability of the oxide to maintain a high dispersion of chromium.

A number of observations with bearing on this matter have been made. DeRossi *et al.* [7] reported similar activation energies for the catalytic dehydrogenation over Cr/alumina, Cr/silica and chromia. About ten years earlier, Lugo and Lunsford [12] observed similar turnover frequency per chromium atom on alumina and silica. This was interpreted in terms of similar active species on these oxides. [12, 13]

On the other hand, chromium clearly has different redox properties on silica compared to on alumina. If the calcined Cr/oxide sample is reduced with carbon monoxide, silica primarily stabilizes Cr(II) while alumina favors Cr(III) species. On a mixed silica/alumina support, Weckhuysen *et al.* [9] observed the catalytic activity to increase linearly with the amount of pseudo-octahedral Cr(III), which correlates with the alumina contents. DeRossi *et al.* [7] selectively oxidized Cr(II)/silica to Cr(III)/silica by using steam. The resulting catalytic activity was taken as proof of catalytically active Cr(III) species on silica. [7]

While these findings show that Cr(III) species are most likely active with respect to catalytic dehydrogenation of alkanes on both silica and alumina, a contribution from Cr(II)/silica should not be ruled out. Early workers ascribed all activity on the CO-reduced Cr/silica to Cr(II), [12] whereas Hakuli *et al.* [14] found Cr(II) active, though less so than Cr(III). A common observation is that isolated species of Cr(II) on silica are quickly deactivated by coking. [12, 14]

Amorphous chromia starts to form with increasing chromium load. Another property that make a distinction between oxide carriers is their ability to disperse Cr(III) oxide. On alumina, α-Cr_2O_3 particles are observed only at chromium loadings above 6-7 wt% chromium, [1, 8, 13, 15] while on silica, α-Cr_2O_3 particles appear already at 2-3 wt%. [16–18] Below 2 wt% chromium on alumina, silica and zirconia, the activity increases linearly with the chromium load, indicating mononuclear active species. [1, 7, 8, 19, 20] On the other hand, the high activity of Cr/alumina at chromium loadings well above monolayer coverage, indicates the presence of highly active sites also on polynuclear amorphous Cr(III) oxide. [13, 15, 21–23] In fact, one explanation that has been offered to differences in activity between Cr/alumina, Cr/silica, and Cr/zirconia, is the difference in ability to stabilize amorphous Cr(III) oxide. [10, 11]

Although surface sites of polynuclear chromium species appear highly active, reaction kinetics on Cr/alumina suggest a mechanism involving single, coordinatively unsaturated chromium centers. [24] What may seem like a paradox is resolved by the realization that chromium atoms neighboring on a reactive chromium center may take on the same function as neighboring aluminum or silicon atoms. This corroborates what appears to be a growing consensus in the literature, that differences in catalytic activity between the oxides stem largely from the ability to stabilize the active species. Building on this hypothesis, it is useful to combine observations made on different supports to encroach on the supposedly common

active species.

Combined reactivity and spectroscopy studies of Cr/silica, [7, 25] led DeRossi *et al.* to propose that the active Cr(III) species has two coordinative vacancies. The species was depicted as bonded to the surface *via* two oxygen bridges and with hydroxyl as the third ligand. [7] ¿From its spectroscopic signature, the species was dubbed Cr(III)G. In several studies we have used quantum chemical modeling to explore the properties of this site and generalizations of it, with respect to catalytic dehydrogenation of ethane. [26, 27] Several reaction mechanisms have been explored, based on C–H activation by either σ-bond metathesis [26] or oxidative addition. [27] The results may be briefly summarized as follows. σ-bond metathesis appears as the favored mechanism for dehydrogenation on this system. Depending on the nano-range surrounding the active site, dehydrogenation can occur either according to a cycle composed of the reaction steps shown schematically as (**1**,**2**,**3**) in Fig. 1, or according to the energetically favored (**4**,**2**)-cycle, shown in the same figure. The initial metathesis steps in the two competing cycles involve a Cr–O (**1**) and a Cr–H bond (**4**), and accordingly we will refer to the two mechanisms as σBM/CrO and σBM/CrH, respectively. Reflecting the strength of the Cr–ligand bond cleaved in the C–H activation step, the computed activation energy of the σBM/CrO mechanism exceeds that of the σBM/CrH mechanism by more than 100 kJ/mol. However, the σBM/CrH mechanism owes its possible existence to reaction **1** being irreversible and reaction **3** in Fig. 1 being prevented. These conditions put constraints on the admissible nano-range surrounding the active site.

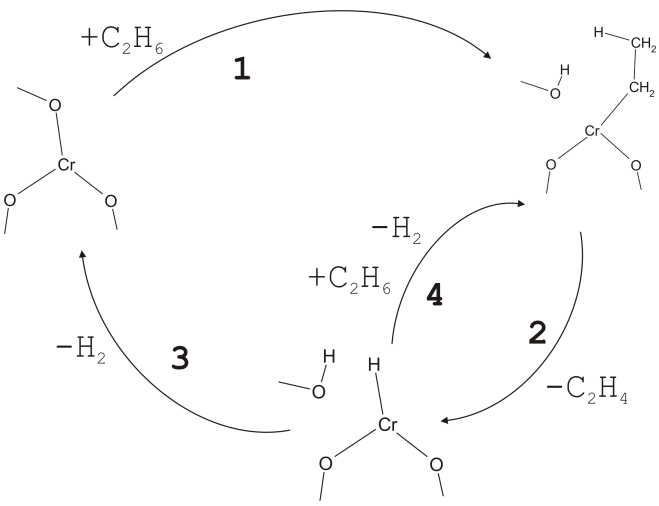

FIG. 1: Schematic reaction mechanisms for dehydrogenation of ethane over Cr/silica as initiated by σ-bond metathesis. The (1,2,3) cycle was proposed by Weckhuysen and Schoonheydt, [1] and the reverse cycle was suggested by Burwell *et al.* in 1960 [28] for hydrogenation of ethene. The (4,2) cycle was first suggested in Ref. [26].

The hypothesis that the difference in catalytic activity between the oxides stems largely from differences in their ability to stabilize the active species, presupposes that functionally equivalent chromium species are responsible for dehydrogenation on all the Cr/oxide systems, and, moreover, that the same reaction mechanism is at work. In this contribution we use quantum chemical modeling to explore whether the two metathesis-based reaction mechanisms earlier found to be viable for dehydrogenation of ethane over Cr/silica, perform equally well on Cr/alumina and chromia. To this end, we use clusters models of mono- and polynuclear Cr(III) surface species that are triply coordinated through oxygen and anchored to the surface *via* two or three Cr–O–M linkages, where M=Si, Al and Cr.

II. COMPUTATIONAL MODELS AND METHODS

On both alumina and silica, chromium is anchored to the support in reactions with surface hydroxyl groups to give Cr–O–M linkages, M=Si, Al. [10, 13, 29–33]. The hydroxyl groups on surfaces of hydrated silica are of the type HO(-Si)$_1$, i.e. with oxygen coordinating to one silicon atom. [34] On hydrated alumina, the hydroxyl groups are of two kinds, HO(-Al)$_1$ and HO(-Al)$_2$, with oxygen coordinating to one or two aluminum atoms, respectively, see Ref. [35] and the references therein. Chromium anchored by reaction with these surface groups would give Cr-O(-M)$_1$ and Cr-O(-M)$_2$ linkages with doubly- and triply-coordinated oxygen in the bridges, respectively. These bonding patterns are represented in the current set of cluster models of Cr(III)/oxide presented in Fig. 2.

The 2bridge-alumina model in Fig. 2**A** represents a hydroxychromium(III) species on an anchoring site with two doubly coordinated oxygen linkages on the (100) face of γ-alumina. The model is a modification of a Mo/alumina cluster used to study ethene metathesis. [36] In the original study, Handzlik *et al.* used clusters of different sizes to represent a surface site with two vicinal HO(-Al)$_1$ groups. Based on the chemical properties of the HO(-Al)$_1$ groups, they decided that the present cluster gave a sufficient representation of the site. [36] The 2bridge-alumina model in Fig. 2**A** is obtained by linking a Cr(OH)$_3$ molecule to the surface site by a condensation reaction, followed by optimizing the geometry to a minimum on the potential energy surface. Structural parameters describing the active chromium center are included in Tab. I.

The 3bridge-alumina model shown as Fig. 2**E** represents a chromium(III) species anchored *via* triply coordinated oxygen to the (001) face of α-alumina. The model is a modification of a V/alumina cluster used by Magg *et al.*, [37] who started out from a Al_8O_{12} cluster cut from the (001) surface of α-alumina and replaced an aluminum atom at the surface by a V=O moiety. We replaced the V=O group by a chromium atom and reoptimized the structure of the resulting cluster.

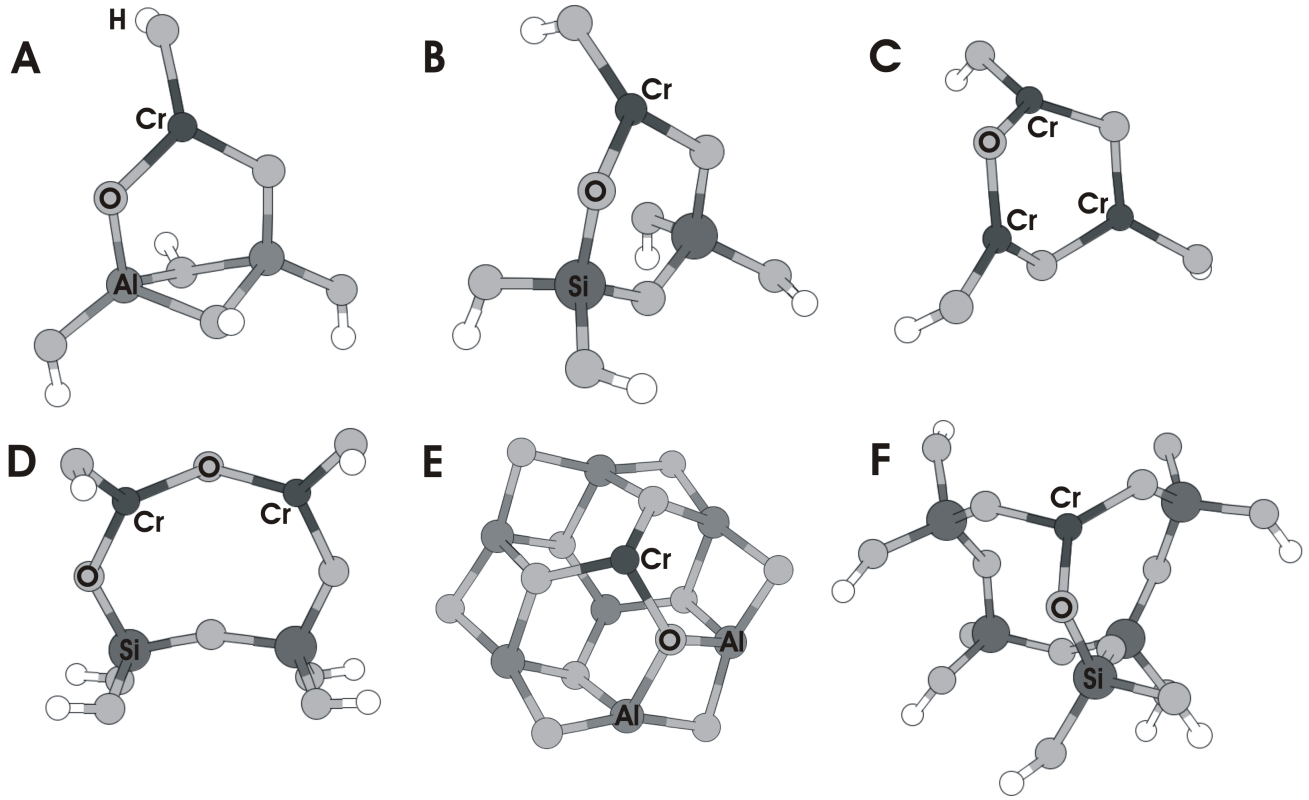

FIG. 2: Models of Cr(III)/oxide surface species: 2bridge-alumina (**A**), 2bridge-silica (**B**), 2bridge-chromia (**C**), diCr-silica (**D**), 3bridge-alumina (**E**), and 3bridge-silica (**F**).

The 2bridge-chromia model in Fig. 2**C** is constructed to be a simple model of a polynuclear chromium site on amorphous chromia. The model is composed of three hydroxychromium(III) centers linked by Cr–O–Cr bridges with twofold coordinated oxygens, and the geometry relaxed to a minimum on the potential energy surface. One or more of the hydroxyl groups may be viewed as a severed Cr–O–M linkage, M=Al, Si, Cr depending on the support, where the dangling bond has been terminated with hydrogen.

The diCr-silica model in Fig. 2**D** represents a site of dinuclear chromium on a silica surface. The two hydroxychromium(III) centers are separated by a Cr–O–Cr linkage, and each chromium center is anchored to a surface silicon *via* doubly coordinated oxygen. The silica surface site is represented by a disiloxyether; the more distant parts of the silica being neglected and the dangling bonds terminated with hydrogen.

Two models are used to represent mononuclear Cr(III) on silica; 2bridge- (**B**) and 3bridge-silica (**F**) where chromium is bonded to the support by two or three oxygen bridges, respectively. These models have been used in previous studies of mononuclear chromium sites and are presented in detail in Ref. [26]. In Ref. [26], cluster **B** was referred to by the name *DeRossi-1*, while cluster **F** was dubbed *(101)-3bridge*. Structural parameters are summarized in Tab. I.

When modeling catalytic dehydrogenation over the 2bridge- and 3bridge-alumina clusters, the structures have been fully optimized for the various reaction steps. The restoring forces of the alumina surface appear well represented in the cluster models of the surface sites. The same approach is used for the 2bridge-chromia model shown as Fig. 2**C**, thus allowing the CrOCr linkages to make full impact on the reactivity. For the diCr-silica model shown as Fig. 2**D**, however, the disiloxyether base is kept frozen to mimicry the restoring forces of a silica surface. In the 3bridge-silica model, the terminating $Si(OH)_2$ groups were held in fixed positions.

TABLE I: The local geometry about the active chromium center in the clusters in Fig. 2.

Cluster	∠OCrO[a]	rCrO[a]
2bridge-alumina (**A**)	123.8, 123.7, 110.3	1.80, 1.80, 1.80
2bridge-silica (**B**)	123.9, 123.9, 107.7	1.81, 1.81, 1.78
2bridge-chromia (**C**)	122.0, 121.9, 114.4	1.79, 1.79, 1.80
diCr-silica (**D**)	117.9, 119.9, 121.6	1.82, 1.79, 1.79
3bridge-alumina (**E**)	102.8, 102.8, 103.1	1.80, 1.80, 1.80
3bridge-silica (**F**)	130.3, 118.0, 110.4	1.83, 1.82, 1.77

[a]Units: Bond lengths (r) in Å, angle (∠) in degrees.

Quantum mechanical calculations have been performed using density functional theory as implemented in the Amsterdam Density Functional (ADF) set of programs [38–40]. For electron correlation the LDA functional of Vosko *et al.* [41] augmented by the nonlocal 1986 corrections by Perdew [42] were used. The exchange functional consists of the Slater term augmented by gradient corrections as specified by Becke [43]. For details of basis sets and geometry optimization see Ref. [26].

In general, energy differences refer to electronic degrees of freedom only, i. e. without zero-point vibrational energies or temperature effects. In order to take into account temperature and entropy effects, the full set of thermodynamic functions were computed in the harmonic and rigid-rotor approximation for simulations based on the 2bridge-alumina surface model. Maximal accuracy of the numerical integration schemes was used. All stationary structures display an ultra-soft vibrational mode which consistently has been omitted from the harmonic analysis.

III. RESULTS

Our earlier investigations of mononuclear Cr(III)-sites on silica suggest that dehydrogenation of ethane may be initiated by σ-bond metathesis involving a C–H bond in ethane and a Cr–ligand bond. [26, 27] In the σBM/CrO mechanism, the active Cr–ligand bond form part of an oxygen bridge between the metal and the support, hence the name. In the competing σBM/CrH mechanism, a reactive chromium hydride must be formed, most likely from a chromium hydroxide precursor. In the following, results for the two mechanisms will be given in some detail for chromium on alumina which, from the industrial point of view, is the most interesting of the Cr/oxide systems. Next, reaction energies are presented for chromium supported on other oxides and used to discuss the role of the support.

In the initial reaction between gas-phase ethane and the 2-bridged Cr/alumina model **A**, a C–H bond may be severed in a metathesis reaction involving either the Cr–OH bond or one of the Cr–OAl linkages. In either case, an ethyl ligand is added to chromium; the difference lies in the formation of a water molecule, in reaction **1a** in Fig. 3, or a surface hydroxyl group according to reaction **1b** in the same figure. Judged from the computed enthalpies of activation, which are given in Tab. II as 146 and 138 kJ/mol, respectively, the two reactions are equally feasible.

A. The σBM/CrH mechanism on alumina

In the primary product of reaction **1a** in Fig. 3, a water molecule remains bound to chromium. However, at a reaction temperature of 500°C, which is realistic for these systems, the increase in entropy upon decoordination of water far outweighs the binding enthalpy. The free energy of desorption becomes -64 kJ/mol, which means that water is released. In the case of moisture-free feed of ethane, reaction **1a** may thus be regarded as irreversible.

This sets the stage for the σBM/CrH mechanism, illustrated at the top of Fig. 3. Starting from the product of **1a**, reaction **2a** involves β-hydrogen transfer from the ethyl ligand to the metal, thus forming a π-bonded hydridochromium–ethene surface complex. The energy increases almost all the way to this primary product and desorption of ethene must follow immediately to prevent the revers reaction. The point of maximum free energy is associated with desorption of ethene, and upper limits to the enthalpy and free energy of activation may be estimated by adding the electronic binding energy of ethene to the energy of the π-bonded hydridochromium–ethene complex. Relative to the ethylchromium reactant complex, the effective enthalpy of activation becomes

TABLE II: Changes in thermodynamic functions (kJ/mol) at 500°C and 1 atm for the reaction steps shown in Fig. 3 for the 2bridge-alumina model (**A**). All values are relative to those for reactants in the same reaction step. The notation includes only atoms that are active in each reaction step.

	ΔE_{elec}	ΔH	ΔG
1a: CrOH + C_2H_6 → Cr(Ethyl) + H_2O(g)			
TS	150	146	260
Cr(Ethyl)(H_2O)	72	83	193
Products	129	128	129
The σBM/CrH cycle:			
2a: Cr(Ethyl) → CrH + C_2H_4			
TS	97	84	92
CrH(C_2H_4)	88	81	73
TS_{eff}	126	119[a]	111[a]
Products	126	107	-15
4: CrH + C_2H_6 → Cr(Ethyl) + H_2(g)			
TS	90	88	206
Products	32	30	46
The σBM/CrO cycle			
1b: Cr–OAl + C_2H_6 → Cr(Ethyl) + AlOH			
TS	143	138	256
Product	89	99	198
2b: Cr(Ethyl) → CrH + C_2H_4(g)			
TS	86	73	86
CrH(C_2H_4)	76	69	72
TS_{eff}	115	108[a]	111[a]
Product	115	96	-19
3: Cr(H) + AlOH → Cr–OAl + H_2(g)			
TS	43	28	43
Product	-46	-58	-148

[a]Estimated by adding the electronic binding energy of ethene to the enthalpy and free energy of the π-bonded hydridochromium–ethene complex.

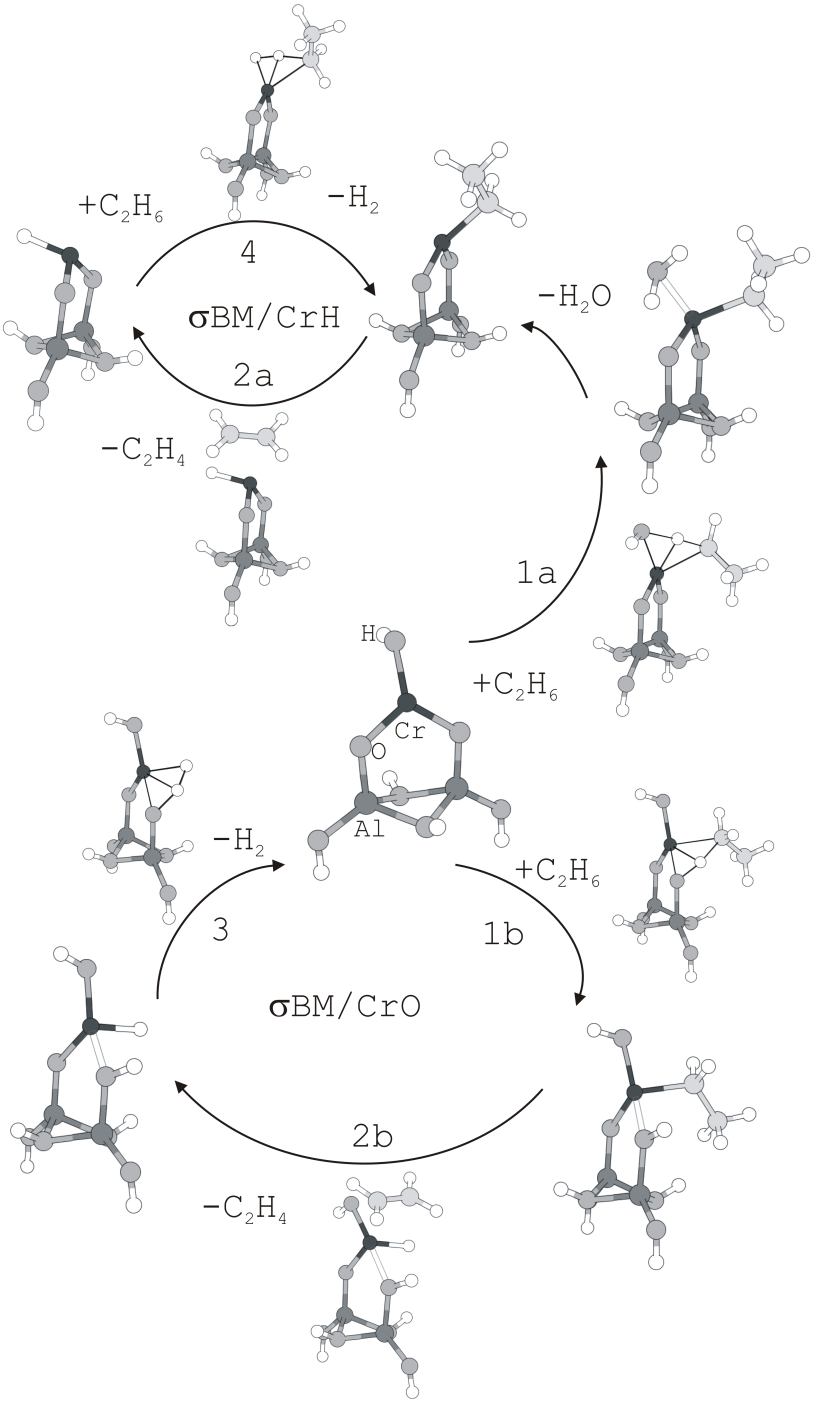

FIG. 3: Optimized stationary structures for the dehydrogenation reaction of ethane over the 2bridge-alumina model catalyst. The reaction steps are (**1a**) C–H activation of ethane by σ-bond metathesis at the Cr–OH bond with subsequent loss of water, (**1b**) C–H activation of ethane by σ-bond metathesis at a Cr–OAl bond, (**2a**, **2b**) β-H transfer to chromium with subsequent loss of ethene, (**3**) Cr–O formation with subsequent loss of H_2, and (**4**) C–H activation of ethane with subsequent loss of H_2.

119 kJ/mol, cf. Table II. Due to the gain in entropy when ethene enters the gas phase, the net free energy change for reaction **2a** comes out negative by 15 kJ/mol.

The hydridochromium complex formed in reaction **2a** may react with a second ethane according to reaction **4**. The Cr–H bond and one of the C–H bonds in ethane are replaced by two new σ bonds, Cr–Ethyl and H–H. H_2 desorbs to the gas phase and the ethylchromium complex appearing as reactant in **2a** is regenerated. While **1a** and the first pass of reaction **2a** may be viewed as ac-

tivation of the site, repeated cycles of **4** and **2a** constitute the σBM/CrH mechanism for catalytic dehydrogenation. ¿From this perspective, it is useful to consider the free energy change with free ethane and the hydridochromium complex are reference states, cf. Fig. 4. The differences in energies between the right and left end points of the graphs in Fig. 4, correspond to the reaction enthalpy and free energy of the net reaction $C_2H_6 \rightarrow C_2H_4 + H_2$. Reaction **4** is clearly the rate-determining step, with enthalpy and free energy of activation of 88 and 206 kJ/mol, respectively.

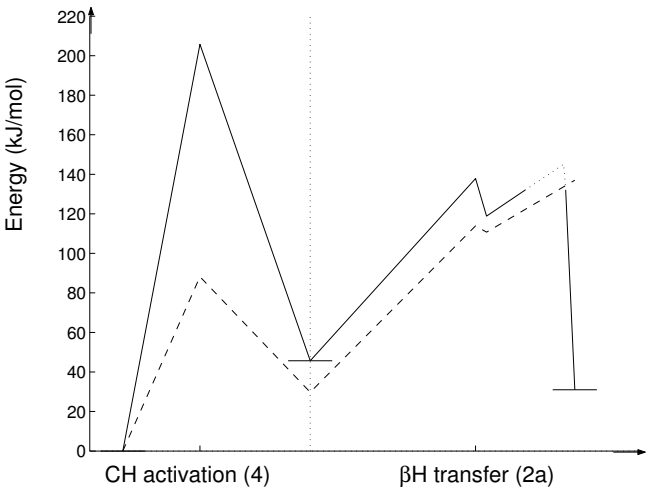

FIG. 4: Free energy (full line) and enthalpy (dashed line) profiles of the σBM/CrH mechanism, the (**4**,**2a**) cycle shown in the upper part of Fig. 3 for dehydrogenation of ethane over the 2bridge-alumina hydridochromium model (**A**) without a spectator water ligand present. A dotted line is used to represent the maximum free energy barrier of ethene desorption. Free energies are given in kJ/mol relative to that of separated ethane and the hydridochromium model catalyst. The reaction steps are (**4**) C–H activation of ethane with subsequent loss of H_2, and (**2a**) β-H transfer to chromium with subsequent loss of ethene.

B. The σBM/CrO mechanism on alumina

Returning to the 2bridge-alumina site at the center of Fig. 3, C–H activation according to **1b** constitutes the first out of three steps in the σBM/CrO mechanism of dehydrogenation. Simultaneously with the formation of a chromium ethyl complex, one of the oxygen bridges that link chromium to the alumina surface is converted into a surface hydroxyl. While polar-covalently bonded to aluminum, the hydroxyl moiety forms a weak dative bond to chromium, taking on a role similar to that of water in reaction **1a**. This is reflected in the Cr–OH distance of 2.22 Å, which is close to the Cr–OH_2 distance of 2.26 Å.

The subsequent β-hydrogen transfer from ethyl to the metal (reaction **2b** in Fig. 3) closely follows the path of its analogue in the σBM/CrH mechanism, **2a**. Desorption of the thus formed ethene is required in order to prevent the reverse reaction from taking place and the effective activation energy is estimated as described for **2a**. The resulting enthalpy of activation relative to that of the reactant ethylchromium complex, is 108 kJ/mol, cf. Table II. Due to the gain in entropy as ethene enters the gas phase, the net free energy change for reaction **2b** comes out negative by 19 kJ/mol.

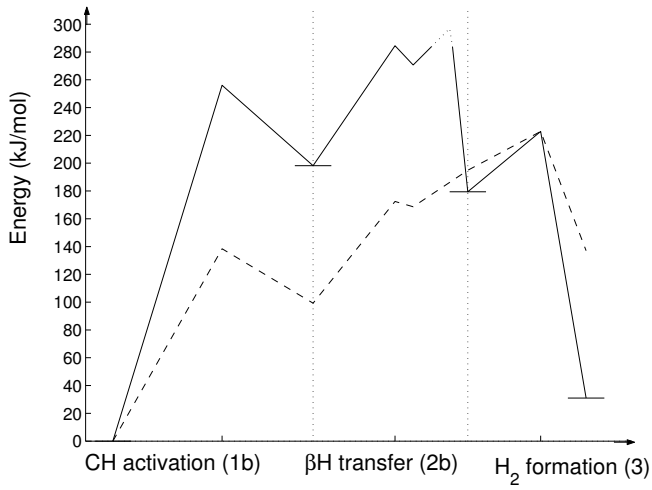

FIG. 5: Free energy (full line) and enthalpy (dashed line) profiles of the (**1b**,**2b**,**3**) cycle shown in Fig. 3 for dehydrogenation of ethane over the 2bridge-alumina model (**A**). A dotted line is used to represent the maximum free energy barrier of ethene desorption. Energies are given in kJ/mol relative to that of separated ethane and the model catalyst. The reaction steps are (**1b**) C–H activation of ethane, (**2b**) β-H transfer to chromium with subsequent loss of ethene, (**3**) Cr–O formation with subsequent loss of H_2.

With the hydroxyl moiety formed in reaction **1** remaining near chromium, the σBM/CrO mechanism may be completed according to reaction **3** in Fig. 3. The Cr–OAl bond is reforged as H_2 gets released to the gas phase. The enthalpy and free energy of activation are 28 and 43 kJ/mol, respectively, relative to the hydridochromium complex after desorption of ethene, cf. Tab. II

The free-energy profile of a full cycle of the σBM/CrO mechanism is plotted in Fig. 5. Apparently, the formation of ethene and a surface hydridochromium complex according to **2b** is the rate-determining step. Relative to energies of ethane and the reactant cluster, the enthalpy and free energy of activation are computed to 207 and 309 kJ/mol, respectively. These numbers are about 100 kJ/mol higher than the corresponding ones for the σBM/CrH mechanism, showing how the latter would be preferred unless deactivated by moisture.

TABLE III: Changes in electronic energy (ΔE_{elec}, in kJ/mol) for the σBM/CrH cycle using models shown in Fig. 3. The notation includes only atoms that are active in each reaction.

	A: 2-bridge alumina	**B**: 2-bridge silica	**C**: 2-bridge chromia	**D**: diCr silica
	1a: CrOH + C_2H_6(g) → CrEthyl + H_2O(g)			
TS[a]	150	138	125	140
CrEthyl(H_2O)[a]	72	66	76	75
Product[a]	129	135	108	118
	4: CrH + C_2H_6(g) → CrEthyl + H_2(g)			
TS[b]	90	71	94	91
Product[b]	32	23	33	28
	2a: CrEthyl → CrH + C_2H_4(g)			
TS[b]	129	110	137	135
CrH(C_2H_4)[b]	119	106	136	132
Product[b]	158	158	158	158

[a]Values are relative to those of the reactants in **1a**.
[b]Values are relative to those of the reactants in **4**.

C. Comparison between Cr(III) on alumina, chromia and silica supports

By comparing energies for the two-bridged alumina model **A** to those given for the analogous silica model (**B**) in Ref. [26], we find that changes in pressure-volume work, zero-point vibrational energies and entropy are fairly transferable between the models. This means that, while drawing on our identification of rate-determining steps from free energies for models **A** and **B**, we may compare the supports on the basis of electronic energies rather than enthalpies or free energies.

1. The σBM/CrH mechanism

Tab. III lists electronic energies computed for models of Cr(III) on alumina, chromia and silica, for reaction steps that either initiate or appear explicitly in the proposed σBM/CrH mechanism for dehydrogenation. In the case of silica, both dinuclear and mononuclear sites are considered.

In the initial **1a** metathesis reaction, activation energies are in the range of 125-150 kJ/mol for all models considered, with chromia and alumina representing the lowest and highest value, respectively. The differences are small, however, and activation seems thus to be facile on all supports.

Turning to the two segments of the catalytic cycle, the reaction energies computed for both the metathesis step **4** and hydrogen transfer (**2a**, *vide infra*) show that the relative strength of the Cr–H and Cr–ethyl bonds is common to all the different surface sites **A**-**D**. Moreover, the electronic activation energies are remarkably independent of the choice of support and also of the nuclearity of the site. For the rate-determining step **4**, three of the four models, representing alumina (**A**), chromia (**C**) and dichromium/silica (**D**) give rise to activation energies between 90 and 94 kJ/mol. Moreover, the same three models give similar activation energies also for the hydrogen transfer reaction **2a**, ranging from 119 to 135 kJ/mol. Contrary to this, the two-bridged Cr/silica model (**B**) gives rise to reaction barriers that arelower than those obtained for the 2bridge-alumina model. This model distinguishes itself by having a particularly narrow $\angle OCrO$ angle between the oxygen bridges. This leaves more space for the four-coordinated transition states and also the primary products that possess dative ligands. Expanding the silica model to three siloxide units as described in Ref. [26], the $\angle OCrO$ angle opens up and the activation energies for reactions **4** and **2a** are brought into agreement with the other models. Hence, while a geminal chromium site of silica may show somewhat enhanced activity, this is due to angular strain rather than direct electronic effects involving the silica.

2. The σBM/CrO mechanism

From the free energy profiles in Figs. 4 and 5, it appears that in order for the σBM/CrO mechanism to become competitive, the chromium-support interaction has to change considerable from that of alumina, to lower the free energies of reactions **1b** and **2b** by 50-100 kJ/mol. Since the initial step in the σBM/CrO mechanism is breaking a Cr-OM bond (M= Al, Cr or Si), one may expect larger differences between the supports than found for the hydride mechanism, which is activated by breaking a Cr–OH bond. To examine this possibility, we have explored the σBM/CrO mechanism on four additional surface models including two-bridged silica (**B**) and chromia (**C**), and two models with chromium bonded to either alumina (**E**) or silica by three oxygen bridges (**F**).

According to Tab. IV, reaction **1b** requires essentially the same activation energy on all five surface models. The only apparent difference lies in the stability of the resulting ethylchromium complex. This is notably less stable on silica than on alumina and chromia, part of which may be due to lack of surface relaxation in the silica models.

Going beyond the energetics, the σ-bond metathesis step takes a somewhat different course on the chromia model than on the other oxides. For simplicity, we will use a prime to distinguish chromium atoms that are regarded as part of the support, from the "active" chromium. As a hydrogen atom gets abstracted from ethane and transferred to the CrOCr′ oxygen bridge, an O–H bond is formed at the expense of the O–Cr′ rather than the Cr–O bond. The ethylCr–O(H)Cr′ distance remains relatively short at 1.92 Å, while the

TABLE IV: Changes in electronic energy (ΔE_{elec}, in kJ/mol) for the σBM/CrO cycle as obtained for various models shown in Fig. 3. All values are relative to those of the reactants in **1b**. The notation includes only atoms that are active in each reaction. M is used to denote the electropositive element in the oxide, Al, Si or Cr as applies.

	A: 2-bridge alumina	**B**: 2-bridge silica	**C**: 2-bridge chromia	**E**: 3-bridge alumina	**F**: 3-bridge silica
	1b: CrOM– + C_2H_6(g) → CrEthyl + HOM–				
TS	143	151	145	146	161
Product	89	120	80	87	109
	2b: CrEthyl → CrH + C_2H_4(g)				
TS	175	198	191	-[a]	209
CrH(C_2H_4)	165	191	179	-	217
Product	204	225	196	245	246
	3: CrH + HOM– → CrOM– + H_2(g)				
TS	247	249	262	262	279
Product	158	158	158	158	158

[a]A proper transition state was not found.

ethylCrO(H)–Cr′ distance lengthens to 2.03 Å. Spin densities of 3.0-3.2 e are found for chromium on the silica and alumina models, consistent with oxidation state +III. On the 2bridge-chromia model, however, an electron spin of 2.38 e is localized on the ethylchromium center, and 3.65 e on Cr′, corresponding to a mixed-valence Cr(IV)Cr′(II) state. The mixed-valence state is found also for the hydrido product of reaction **2b**, while the site reverts to a Cr(III)Cr′(III) configuration at the transition states of reactions **1b** and **2b** and also in the CrH(C_2H_4) π complex. Clearly, a chromium(III) site of nuclearity two has an element of flexibility not present for mononuclear sites. The energy consequences of this internal redox process is difficult to ascertain since the present single-determinant description does not take interaction between the III-III and IV-II configurations explicitly into account. With that reservation, the energy profile that we have obtained for the dehydrogenation reaction is very similar to those found for the mononuclear chromium sites.

For the second, rate-determining reaction **2b**, it is useful to consider sites with two oxygen bridges to chromium separate from those with three bridges. For the first three chromium models, the electronic energy profiles are within 20 kJ/mol of each other, i.e. equal within the accuracy of the theory. In light of the considerable difference in coordination mode of the hydroxyl ligand between chromia on the one hand, and alumina and silica on the other, this shows that the hydrogen transfer step is very local in nature.

On the three-bridge alumina model (**E**), C–H activation over any of the three Cr–O(Al)$_2$ bonds gives an ethylchromium complex with strong β-agostic interactions. This interaction is strong enough to lengthen the C–H$_\beta$ bond to 1.14 Å and to make the eclipsed conformation of ethyl more stable than the non-agostic staggered one, by about 20 kJ/mol. This is contrary to what is found for the other models, where the non-agostic structure with a staggered ethyl is the most stable configuration. While the subsequent β-hydrogen transfer step on **E** is clearly assisted by the agostic interaction, the resulting hydridochromium complex is still higher in energy by 40 kJ/mol compared to its analogue on the 2bridge-alumina model, cf. Tab. IV. These apparently contradicting observations may be understood in light of the Mulliken charge on chromium, which throughout the σBM/CrO cycle remains higher and changes less on the three-bridge alumina model than on any of the other models. Firstly, the high positive charge accounts for the difference in tendency to form agostic structures. Secondly, the product complexes of reactions **1b** and **2b** differ from the unperturbed cluster by having one -OAl ligand replaced by less electronegative ligands. The stability of the Mulliken charge demonstrates that the two intact Cr–OAl bonds in **E** are more effective at absorbing electrons that become available from these replacements, than are the Cr–OH and Cr-OAl bonds left in **A**. Effectively, at the three-bridge alumina site there are less electrons available at chromium to stabilize transition states and the electron-poor hydrido complex, hence the higher overall activation energy for the σBM/CrO cycle.

Turning to the three-bridge silica site, the energy profile of the σBM/CrO mechanism is equally unfavorable as described for the analogous alumina model. Compared to the two-bridge silica model, the difference is much smaller than for the alumina case. Moreover, since the charge flow during the reaction is similar to that found for models **A** and **B**, the higher activation energy for reaction **2b** on model **F** is more likely due to loss of structural rather than electronic flexibility.

IV. DISCUSSION

Before discussing the chemical implications of the present results, it is useful to examine the validity of the

models used. The cluster-model approach to Cr/silica receives support from our finding in Refs. [26, 27] that the reaction energy profiles obtained show good reproducibility from the simplest $Cr(OH)_3$ model to sophisticated models of Cr/silica. Similarly, in a computational study of ethene metathesis over Mo/alumina, the reaction barrier was found to remain stable over a range of cluster sizes. [36] Kubicki and Apitz [44] and De Vito *et al.* [45] report that small alumina clusters terminated by OH or HOH groups, are adequate for describing adsorption and chemisorption over alumina surfaces.

The higher ionicity in alumina as compared to silica warrants an assessment of our neglecting the long-range electrostatic field. Initiation of the σBM/CrH mechanism requires that the water formed in reaction **1a**, desorbs. The Madelung field has been shown to contribute about 20 kJ/mol to the adsorption energy of molecular water on surface aluminum ions of alumina. [46, 47] While this appears to be an upper limit to what one might be expected for the coordination energy of water on CrO_x species dispersed on alumina, it would still leave the free energy of desorption of water negative by 30-50 kJ/mol at 500°C. As far as activation energies are concerned, it is instructive to consider dissociation of water on Al–O pairs on models of alumina surfaces. This may be considered a high-polarity analogue of reaction **1** in Fig. 1, thus presenting a worst-case scenario. Inclusion of the Madelung field was found to destabilize the energy of the dissociative product by about 20 kJ/mol relative to the reactant asymptote. [46, 47] Although we expect the neglect of the long-range potentials to impart notably smaller errors than this to the computed energy profiles for the σBM/CrH and σBM/CrO mechanisms, we will confine our discussion to energy differences larger than 20 kJ/mol.

At a hydroxylchromium(III) site bonded to alumina by two oxygen bridges, we find the rate-determining step of the σBM/CrH mechanism to involve an enthalpic barrier of 88 kJ/mol, corresponding to a free energy of activation of 206 kJ/mol. At the same site, the rate-determining step of the σBM/CrO mechanism involves an enthalpy and free energy of activation of 207 and 309 kJ/mol, respectively. These numbers agree well with those previously reported for Cr(III)/silica. [26] Indeed, the gross features of the reaction energy profiles computed for both the σBM/CrH and the σBM/CrO mechanisms of dehydrogenation appear largely independent of the choice of alumina, silica or chromia as support material, and also of the nuclearity of chromium on silica. ¿From the activation energies alone, the σBM/CrH mechanism appears much favored over the σBM/CrO mechanism for the kind of site just described.

Based on the observed reaction kinetics, a number of proposals have been launched with respect to the nature of the rate-determining step, including C–H activation [24] and desorption of ethene. [48, 49] By combining isotope labeling and transient reactions, Olsbye *et al.* [50] made a convincing case for C–H activation as the rate-determining step during dehydrogenation of ethane over a Cr/alumina catalyst. This agrees with our results for the σBM/CrH mechanism.

The σBM/CrH mechanism requires the stabilization of a highly reactive hydridochromium complex. There are observations that suggest this may be possible, such as the detection of chromium hydrides on chromia treated with H_2, [51] reports of synthesis of hydridochromium complexes, [52] and evidence for C–H activation of ethane over silica-supported transition metal hydrides, including chromium hydride. [53–55].

Continuous activity of the σBM/CrH mechanism requires the absence of water or hydroxyl moieties in the vicinity of active hydridochromium species. Even small amounts of water in the feed is known to poison catalytic dehydrogenation. [7, 12] Activation of a three-bridge Cr(III) site is likely to produce a surface hydroxyl in its proximity, and a hydridochromium species would quickly get deactivated in a condensation reaction. For this reason, mono- and polynuclear two-bridge CrOH species as originally proposed by DeRossi *et al.* [7], appear as likely precursors for the active species on silica and alumina.

On supports void of CrOH structures, the σBM/CrH mechanism is not expected to operate. This may open for the σBM/CrO mechanism, which according to Tab. IV implies an activation energy of about 250 kJ/mol. Clearly, this means a drastically lowered activity, although some of this may be compensated for by the higher density of active chromium sites. Crystalline α-chromia is an example in mind where chromium centers at the surface have at least three oxygen bridges. Still, real samples will have a varying degree of defect formation, making the surface increasingly amorphous and allowing the formation of two-bridge CrOH centers. These ideas receive some support from experiments. König and Tétényi [49, 56] reported an activation energy of 180 kJ/mol for the dehydrogenation of ethane over α-chromia, and proposed as rate determining the surface reaction of β-hydrogen transfer. This is consistent with the present results for the σBM/CrO mechanism. On the other hand, other researchers find chromium to be about half as active on α-chromia as it is on silica, [12] suggesting the presence of two-bridge Cr(III) defects on α-chromia. Additional activity data exists for other short alkanes like propane, i-butane and cyclohexane. [7, 10, 13, 14, 24] However, we will not discuss these further, in part because the larger alkanes may open reaction paths that are not available to ethane, and in part because the activation data only confirm the range of and spread in activation energies already presented for ethane.

The computational results presented here clearly favor the σBM/CrH mechanism on two-bridge Cr(III) sites. Given how stable the reaction energy profile is with respect to change of oxide, the role of the support seems primarily one of stabilizing the reactive chromium species or its precursor. In particular, it appears that a success-

ful support should prevent the surface species from reorganizing to structures where chromium is bonded by three or more oxygen bridges. Silica and alumina differ in this respect. On silica, chromium more easily aggregates into crystallites of α-chromia, [10, 14, 16–18] which leaves fewer chromium atoms exposed and of those that are, a considerable fraction is likely to be bonded by more than two oxygen bridges. Alumina, on the other hand, is able to stabilize a layer of amorphous chromia even beyond monolayer loading of chromium. [8, 10, 13, 15] In fact, the formation of polynuclear chromium species may be advantageous if it increases the number of surface chromiumhydroxyls that may become activated. Puurunen *et al.* reported that mononuclear Cr/alumina is less active than polynuclear Cr/alumina. [22] This observation is consistent with beneficial interaction between chromium centers to prevent chromium(III) ions from forming three-bridge chromium species in octahedral vacancies in the alumina surface.

V. CONCLUSIONS

The role of alumina, silica and chromia supports has been studied with respect to the activity of surface chromium(III) species for catalytic dehydrogenation of ethane. The favored route to dehydrogenation of ethane appears to involve C–H activation by σ-bond metathesis on a hydridochromium(III) species. The σ-BM/CrH route appears viable for mononuclear chromium sites on alumina and silica as well as over amorphous chromia. A likely precursor for the hydridochromium(III) species is a CrOH moiety bonded to the surface *via* two CrOM linkages, M= Si, Al or Cr. This implies that polynuclear chromium(III) species may be active for dehydrogenation of alkanes. On this basis, the role of the substrate seems one of stabilizing a reactive hydridochromium complex or a surface chromiumhydroxide precursor.

The enthalpic and free-energy barriers to dehydrogenation are computed to about 100 and 200-250 kJ/mol for all models considered. While there are differences in activation energies in the order of 20 kJ/mol between the supports, at the present level of accuracy this is not regarded as significant. The study lends support to the notion that the same type of chromium species is active on all the studied oxides and acting according to the same reaction mechanism. Observed differences between the oxides may be due to differences in the density of active species and differences in kinetic parameters in the order of 20 kJ/mol in activation energies. The alternative mechanism of σ-bond metathesis over oxygen bridges between chromium and the support, is found to imply significantly higher reaction barriers. Apparently, this mechanism would only be important if reaction conditions prevents the stabilization of surface chromiumhydride species.

Acknowledgments

We thank the Research Council of Norway (NFR) for financial support and for a grant of computer time through the Programme for Supercomputing.

[1] Weckhuysen, B. M. and Schoonheydt, R. A. *Catal. Today* **51**, 223–232 (1999).
[2] Bhasin, M. M., McCain, J. H., Vora, B. V., Imai, T. T., and Pujadó, P. R. *Appl. Catal. A Gen.* **221**, 397–419 (2001).
[3] Hall, M. B. and Fan, H. J. *Adv. Inorg. Chem.* **54**, 321–349 (2003).
[4] Huff, M. and Schmidt, L. D. *J. Phys. Chem.* **97**, 815–822 (1993).
[5] Liebmann, L. S. and Schmidt, L. D. *Appl. Catal. A Gen.* **179**, 93–106 (1999).
[6] Beretta, A., Ranzi, E., and Forzatti, P. *Catal. Today* **64**, 103–111 (2001).
[7] DeRossi, S., Ferraris, G., Fremiotti, S., Garrone, E., Ghiotti, G., Campa, M. C., and Indovina, V. *J. Catal.* **148**, 36–46 (1994).
[8] DeRossi, S., Casaletto, M. P., Ferraris, G., Cimino, A., and Minelli, G. *Appl. Catal. A Gen.* **167**, 257–270 (1998).
[9] Weckhuysen, B. M., Bensalem, A., and Schoonheydt, R. A. *J. Chem. Soc., Faraday Trans.* **94**, 2011–2014 (1998).
[10] Gaspar, A. B., Brito, J. L. F., and Dieguez, L. C. *J. Mol. Catal. A* **203**, 251–266 (2003).
[11] Gaspar, A. B. and Dieguez, L. C. *J. Catal.* **220**, 309–316 (2003).
[12] Lugo, H. I. and Lunsford, J. H. *J. Catal.* **91**, 155–166 (1985).
[13] Cavani, F., Koutyrev, M., Trifirò, F., Bartolini, A., Ghisletti, D., Iezzi, R., Santucci, A., and Piero, G. D. *J. Catal.* **158**, 236–250 (1996).
[14] Hakuli, A., Harlin, M. E., Backman, L. B., and Krause, A. O. I. *J. Catal.* **184**, 349–356 (1999).
[15] Hakuli, A., Kytökivi, A., and Krause, A. O. I. *Appl. Catal. A Gen.* **190**, 219–232 (2000).
[16] Hardcastle, F. D. and Wachs, I. E. *J. Mol. Catal.* **46**, 173–186 (1988).
[17] Fouad, N. E., Knözinger, H., Zaki, M. I., and Mansour, S. A. A. *Z. Phys. Chem.* **171**, 75–96 (1991).
[18] Weckhuysen, B. M., Verberckmoes, A. A., Buttiens, A. L., and Schoonheydt, R. A. *J. Phys. Chem.* **98**, 579–584 (1994).
[19] DeRossi, S., Ferraris, G., Fremiotti, S., Indovina, V., and Cimino, A. *Appl. Catal. A Gen.* **106**, 125–141 (1993).
[20] Hakuli, A., Kytökivi, A., Krause, A. O. I., and Suntola, T. *J. Catal.* **161**, 393–400 (1996).
[21] Airaksinen, S. M. K., Kanervo, J. M., and Krause, A. O. I. *Stud. Surf. Sci. Catal.* **136**, 153–158 (2001).
[22] Puurunen, R. L. and Weckhuysen, B. M. *J. Catal.* **210**, 418–430 (2002).
[23] Puurunen, R. L., Airaksinen, S. M. K., and Krause, A.

O. I. *J. Catal.* **213**, 281–290 (2003).
[24] Airaksinen, S. M. K., Harlin, M. E., and Krause, A. O. I. *Ind. Eng. Chem. Res.* **41**, 5619–5626 (2002).
[25] Ghiotti, G. and Chiorino, A. *Spectrochim. Acta A* **49**, 1345–1359 (1993).
[26] Lillehaug, S., Børve, K. J., Sierka, M., and Sauer, J. *J. Phys. Org. Chem.* **17**, 990–1006 (2004).
[27] Lillehaug, S., Jensen, V. R., and Børve, K. J. *J. Phys. Org. Chem.* **19**, 25–33 (2006).
[28] Burwell, R. L., Littlewood, A. B., Cardew, M., Pass, G., and Stoddard, C. T. H. *J. Am. Chem. Soc.* **82**, 6272–6280 (1960).
[29] Vuurman, M. A., Wachs, I. E., Stufkens, D. J., and Oskam, A. *J. Mol. Catal.* **80**, 209–227 (1993).
[30] Mentasty, L. R., Gorriz, O. F., and Cadús, L. E. *Ind. Eng. Chem. Res.* **38**, 396–404 (1999).
[31] McDaniel, M. P. *J. Catal.* **76**, 17–28 (1982).
[32] Kim, D. S., Tatibouet, J.-M., and Wachs, I. E. *J. Catal.* **136**, 209–221 (1992).
[33] Haukka, S., Lakomaa, E.-L., and Suntola, T. *Appl. Surf. Sci.* **75**, 220–227 (1994).
[34] Sauer, J., Ugliengo, P., Garrone, E., and Saunders, V. R. *Chem. Rev.* **94**, 2095–2160 (1994).
[35] Raybaud, P., Digne, M., Iftimie, R., Wellens, W., Euzen, P., and Toulhoat, H. *J. Catal.* **201**, 236–246 (2001).
[36] Handzlik, J. and Ogonowski, J. *J. Mol Catal. A-Chem.* **175**, 215–225 (2001).
[37] Magg, N., Immaraporn, B., Giorgi, J. B., Schroeder, T., Baumer, M., Dobler, J., Wu, Z., Kondratenko, E., Cherian, M., Baerns, M., Stair, P. C., Sauer, J., and Freund, H.-J. *J. Catal.* **226**, 88–100 (2004).
[38] te Velde, G., Bickelhaupt, F., van Gisbergen, S. J. A., Guerra, C. F., Baerends, E. J., Snijders, J. G., and Ziegler, T. *J. Comput. Chem.* **22**, 931–967 (2001).
[39] Guerra, C. F., Snijders, J. G., te Velde, G., and Baerends, E. J. *Theor. Chem. Acc.* **99**, 391–403 (1998).
[40] Baerends, E. J., Autschbach, J. A., Bérces, A., Bo, C., Boerrigter, P. M., Cavallo, L., Chong, D. P., Deng, L., Dickson, R. M., Ellis, D. E., Fan, L., Fischer, T. H., Fonseca Guerra, C., van Gisbergen, S. J. A., Groeneveld, J. A., Gritsenko, O. V., Grüning, M., Harris, F. E., van den Hoek, P., Jacobsen, H., van Kessel, G., Kootstra, F., van Lenthe, E., Osinga, V. P., Patchkovskii, S., Philipsen, P. H. T., Post, D., Pye, C. C., Ravenek, W., Ros, P., Schipper, P. R. T., Schreckenbach, G., Snijders, J. G., Sola, M., Swart, M., Swerhone, D., te Velde, G., Vernooijs, P., Versluis, L., Visser, O., van Wezenbeek, E., Wiesenekker, G., Wolff, S. K., Woo, T. K., , and Ziegler, T. *ADF 2002.03 Computer Code*, (2002).
[41] Vosko, S. H., Wilk, L., and Nusair, M. *Can. J. Phys.* **58**, 1200–1211 (1980).
[42] Perdew, J. P. *Phys. Rev. B* **33**, 8822–8824 (1986).
[43] Becke, A. D. *Phys. Rev. A* **38**, 3098–3100 (1988).
[44] Kubicki, J. D. and Apitz, S. E. *Am Mineral* **83**, 1054–1066 (1998).
[45] Vito, D. A. D., Gilardoni, F., Kiwi-Minsker, L., Morgantini, P.-Y., Porchet, S., Renken, A., and Weber, J. *THEOCHEM* **469**, 714 (1999).
[46] Shapovalov, V. and Truong, T. N. *J. Phys. Chem. B* **104**, 9859–9863 (2000).
[47] Wittbrodt, J. M., Hase, W. L., and Schlegel, H. B. *J. Phys. Chem. B* **102**, 6539–6548 (1998).
[48] Kao, J.-Y., Piet-Lahanier, H., Walter, E., and Happel, J. *J. Catal.* **133**, 383–396 (1992).
[49] König, P. and Tétényi, P. *Acta Chim. Hung.* **89**, 123–136 (1976).
[50] Olsbye, U., Virnovskaia, A., Prytz, O., Tinnemans, S. J., and Weckhuysen, B. M. *Catal. Lett.* **103**, 143–148 (2005).
[51] Busca, G. *J. Catal.* **120**, 303–313 (1989).
[52] Filippou, A. C., Schneider, S., and Schnakenburg, G. *Angew. Chem. Int. Ed.* **42**, 4486–4489 (2003).
[53] Vidal, V., Théolier, A., Thivolle-Cazat, J., and Basset, J.-M. *Science* **276**, 99–102 (1997).
[54] Maury, O., Lefort, L., Vidal, V., Thivolle-Cazat, J., and Basset, J.-M. *Angew. Chem. Int. Ed.* **38**, 1952–1955 (1999).
[55] Mikhailov, M. N., Bagatur'yants, A. A., and Kustov, L. M. *Russ. Chem. Bull. Int. Ed.* **52**, 30–35 (2003).
[56] König, P. and Tétényi, P. *Acta Chim. Hung.* **89**, 137–150 (1976).